

Controllable Fabrication of Patterned Oblique Nanowire Array and Its Application as a Reflection Grating

Li Cheng¹, Wei Dou^{1,3}, Suo Bai¹, Weiwei Wu¹, Qi Xu¹, and Yong Qin^{1,2,*}

¹Institute of Nanoscience and Nanotechnology, Lanzhou University, 730000, China

²Beijing Institute of Nanoenergy and Nanosystems, Chinese Academy of Sciences, Beijing 100085, China

³School of Chemistry and Chemical Engineering, Lanzhou University, 730000, China

ABSTRACT

Aligned oblique nanostructures are widespread and playing important roles in natural world. However the controllable fabrication of these nanostructures is still a challenge up to now. Here we developed a simple silica nanospheres assisted ion bombarding method to make patterned oblique nanowire (NW) arrays on different substrates such as polyimide (Kapton) film, polyester (PET) film, polyaniline (PANI) film and SU-8 photoresist film. Their obliquity, diameter, wire density and length were well controlled by changing the experimental parameters. By changing the incident angle of Ar⁺ ion beam, NW arrays with oblique angles ranging from 20° to 80° were made, and oblique NW arrays with diameters ranging from 191 to 331 nm were fabricated using different sized silica nanospheres as shadow mask. The density of the silica nanosphere array determined the wire density of the oblique NW array. The bombarding time by Ar⁺ ions was used to control the length of the NW. Finally, the aligned oblique NW array was made into a reflection grating, which showed anisotropic structural color.

KEYWORDS: Oblique Nanostructure, Nanowire Array, Anisotropic Optical Property, Structural Color.

1. INTRODUCTION

As a widespread structure in nature, anisotropic nanostructure has a lot of unique properties and plays an important role in biological systems. Among all those anisotropic nanostructures, well aligned oblique nanostructure is extremely important because of its distinguished mechanical,^{1–3} wetting^{4–8} and optical^{9–12} properties. It is used by dragonflies to lock the head with the back to protect their head when they fly at a very high speed.¹³ Tenebrionid beetles attach their forewings (elytra) to their thorax through interlocking fields of microtrichia (MT) located between thorax and body and between left and right elytra.¹⁴ Water droplets on feather tend to roll off distally because of the tilting barbs on its rachis.¹⁵ The oblique ridges on cover scales of *M. didius* play a significant role in the coloration of the blue wing by anisotropically diffusing the light.¹² Inspired by these natural structures, outstanding properties such as optical anisotropy¹⁶ can be expected if oblique NWs can be fabricated artificially.

Up to now, several methods have been explored to fabricate aligned oblique nanostructures, these structures tilt to a certain side uniformly relative to the normal. Glancing angle deposition has been used to fabricate very dense oblique NWs through a physical vapor deposition process where the deposition flux is incident onto a substrate with a large angle with respect to the normal direction of the surface.^{7,17,18} Sideways physical deposition process is taken to bend vertical NWs into aligned oblique NWs through depositing material on one side of the NWs.^{19–21} Replica molding and subsequent oblique electron beam irradiation is explored to fabricate oblique polymer NWs.^{5,22} Directional ion bombarding method is utilized to make many kinds of robust oblique NW array.²³ But it is still a challenge to control the arrangement, diameters, density of oblique NWs.

In this paper, we report a silica nanospheres assisted ion bombarding (SAIB) method to fabricate patterned oblique NW arrays of different materials such as polyimide (Kapton) film, polyester (PET) film, polyaniline (PANI) film, SU-8 photoresist film etc. Compared with the directional ion bombarding method,²³ the diameter, length, wire density and even arrangement of NWs can be precisely well controlled by changing the size of silica nanospheres and other experimental parameters. And Kapton film with the

* Author to whom correspondence should be addressed.

Email: qinyong@lzu.edu.cn

Received: xx XXXX XXXX

Accepted: xx XXXX XXXX

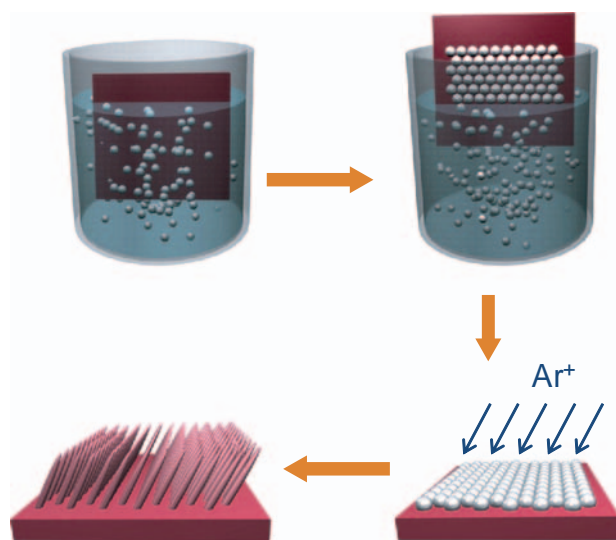


Fig. 1. Schematic of silica nanospheres assisted ion bombardment (SAIB) method for fabricating patterned oblique NW array.

periodically distributed and well aligned oblique NW array is made into a reflection grating, which shows anisotropic structural color because of anisotropic light scattering when light shines on it.

2. FABRICATION OF PATTERNED OBLIQUE NW ARRAY

As shown in Figure 1, the fabrication of patterned oblique NW array through SAIB method could be divided into two steps: First, a uniform monolayer of silica nanospheres is dip-coated²⁴ on the surface of a piece of cleaning polymer film. Then, the film with closely packed monolayer nanospheres is bombarded by Ar⁺ ions with a chosen incident angle for 20 minutes. Due to the difference in etching speed between silica nanospheres and polymer film under bombardment by ion beam, a patterned oblique polymer NW array is formed on the polymer film. Oblique angle of NWs can be controlled by the incident angle of ion beam. And the periodicity and distribution of NWs is determined by that of monolayer silica nanospheres covering the substrate initially. Details of this process can be found in the experimental section.

3. RESULTS AND DISCUSSION

Figure 2(a) shows the scanning electron microscope (SEM) image of monolayer silica nanospheres on Kapton film, which shows that the nanospheres are closely packed on the substrate. After bombarding Kapton film with Ar⁺ ions in 40° incident angle for 5 minutes, well aligned Kapton NWs appear with smaller silica nanospheres on their tops (Fig. 2(b)), which indicates that the monolayer nanospheres act as mask in the fabrication process and determine the distribution of NWs. If Kapton film

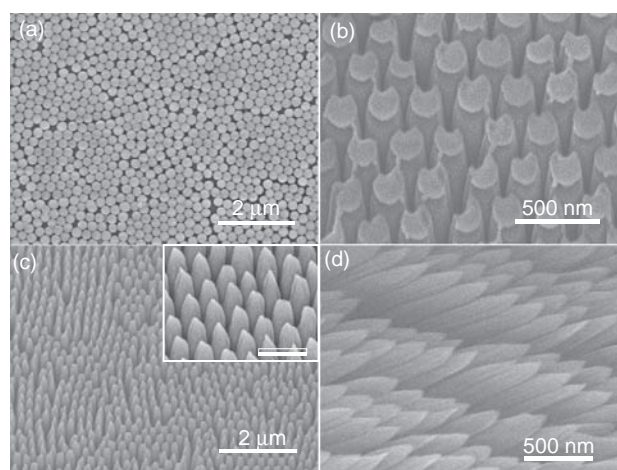


Fig. 2. Scanning electron microscope (SEM) images showing the formation process of 40° oblique Kapton NWs. (a) A monolayer of closely packed silica nanospheres on the surface of Kapton film. (b) Oblique Kapton NW array with residual silica nanospheres on the top, scale bar in the inset is 500 nm, (c) and (d) are top view and sectional view SEM images of fabricated oblique Kapton NW array. Bombarding time of Ar⁺ ions for samples in (b) and (c)–(d) are 5 minutes and 20 minutes respectively.

is continually bombarded by Ar⁺ ions for longer time, silica nanospheres will disappear and oblique NW array forms. Figure 2(c) shows the SEM image of patterned Kapton NW array with the obliquity of 40°. The NWs are quite uniform with diameter of 200 nm. Sectional view shows that NWs are longer than 1 μm and well aligned (Fig. 2(d)). The oblique angle of NWs is about 40° that is equal to the incident angle of Ar⁺ ion beam.

Because any material can be etched by ion bombardment, SAIB method should be a potentially general method to fabricate patterned oblique NW arrays of different materials. To study the general applicability of this method, we attempted to fabricate 40° oblique NW arrays of different polymers. As shown in Figure 3, well aligned oblique Kapton, PET, PANI and SU-8 resist NW arrays can be successfully fabricated. In all cases, the diameter of NWs is determined by the size of silica nanospheres. The length of NWs is determined by ions' bombarding time. And at the same time, the length of NWs is also determined by etching speed of materials under ion bombardment.

For SAIB method, the oblique angle of NW array could be accurately controlled, which is benefit from the directional etching character of ion bombardment. When ions' incident angle less than 20°, NWs connected with each other and connected with the substrate at the bottom, leading to gully-like nanostructures along the incident direction of Ar⁺ ion beam. But when the incident angle of Ar⁺ ion beam is larger than 20°, patterned oblique NW arrays could be fabricated. SEM images of 20° (Figs. 4(a)–(b)), 40° (Figs. 2(c)–(d)), 60° (Figs. 4(c)–(d)) and 80° (Figs. 4(e)–(f)) oblique NW arrays show that the oblique angle of NWs is the same with the incident angle

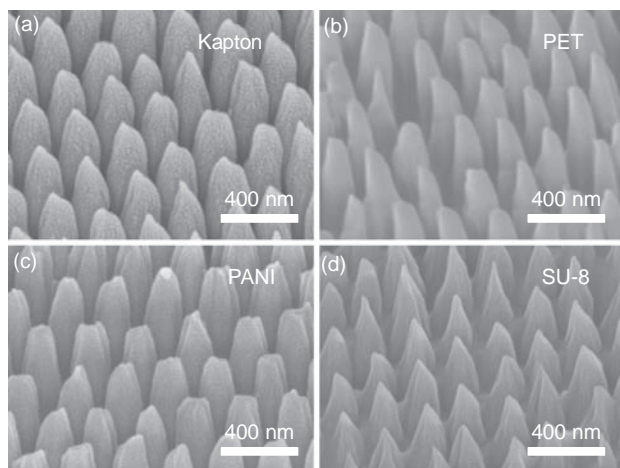


Fig. 3. SEM images of different polymer NWs fabricated by SAIB method. (a) Kapton, (b) PET, (c) PANI and (d) SU-8. Obliquity of all NWs is 40° .

of Ar^+ ion beam. At the incident angle of 20° – 30° , NWs are nearly flat, which is clearly shown in the sectional view of 20° oblique NW arrays (Fig. 4(b)). When incident angle is larger than 30° , cylindrical NW arrays begin to form (as shown in Figs. 4(c)–(f)). The shape changing of oblique NWs with the incident angle of ion beam is probably due to the difference of nanospheres projected on the substrate. The projected area influences the bombarding effect and etching path of Ar^+ ions to the underneath polymer substrate, and finally determines the shape of NWs.

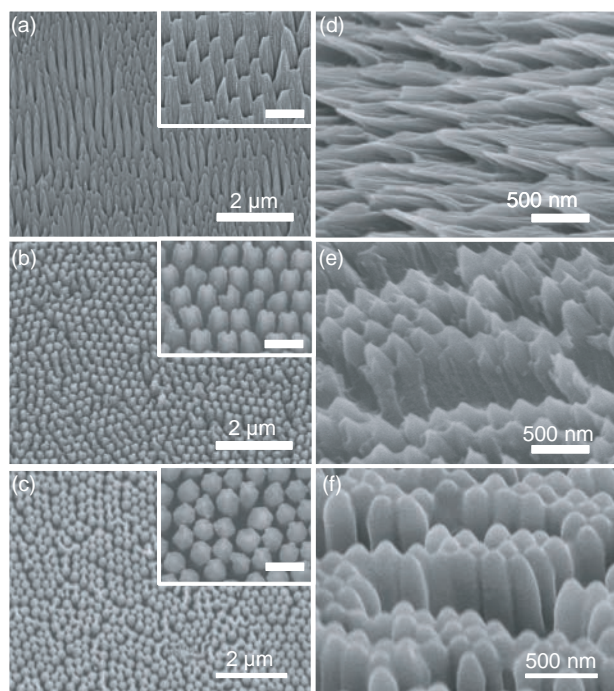


Fig. 4. SEM images of top view (left) and sectional view (right) of different obliquity Kapton NWs. (a), (d) 20° , (b), (e) 60° and (c), (f) 80° . Scale bars in all insets are 400 nm.

In addition to obliquity, the wire density and diameter of NW array could be accurately controlled using monolayers of different sized silica nanospheres as a mask. When larger silica nanospheres are used as monolayer mask, the fabrication processes for all cases are almost the same in our experiment, except for the exception of longer bombarding time. SEM images of NW arrays with different obliquities all show that the distribution of NWs preserves the pattern and density of silica nanosphere monolayer. In addition, using silica nanospheres with diameter of 230 ± 11 , 308 ± 12 , 355 ± 14 and 425 ± 12 nm, NW arrays with average NW diameter of 191 ± 11 , 255 ± 17 , 288 ± 15 and 331 ± 19 nm can be fabricated respectively at 40° Ar^+ incident angle, which are shown in Figures 5(a)–(d). According to statistical results, we plot a graph of NWs' diameter with that of silica nanospheres (Fig. 5(e)), which shows the linear relationship clearly, which indicates that it is easy to control the diameter of NWs.

The surface oblique nanostructure of Kapton film leads to anisotropic optical property. The light scattering property of the patterned 40° oblique Kapton NW array on film was studied in our experiment. In the coordinate system of Figure 6, z direction is perpendicular to film plane, y direction is parallel to the projected direction in film plane of oblique NW, and x direction is perpendicular to

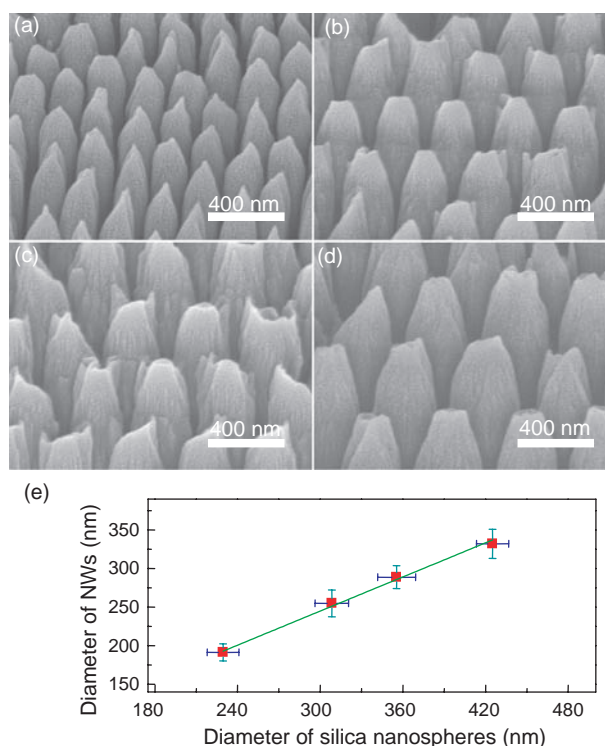


Fig. 5. Diameter control of Kapton NWs by silica nanospheres with different sizes. (a)–(d) SEM images of Kapton NWs fabricated using monolayer mask composed of nanospheres with 230 nm, 308 nm, 355 nm and 425 nm in diameter. (e) The relation between diameter of Kapton NWs and that of silica nanospheres, the error bars show the standard deviations of diameters of silica nanospheres and Kapton NWs.

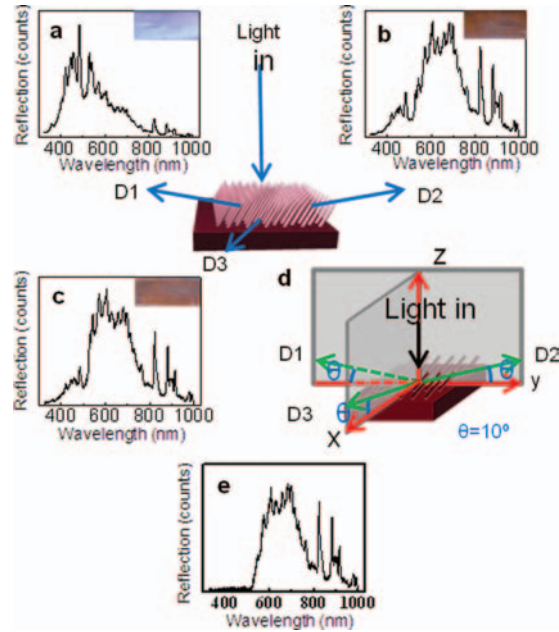


Fig. 6. Anisotropic optical property of oblique NW array on Kapton film. Light shone on the film along the direction— z vertical to film surface. (a)–(c) are the spectra and optical images (insets) observed along $D1$, $D2$ and $D3$ directions. In the coordinate system as shown in (d), z is the normal direction of Kapton film, y is along the projection direction of oblique NWs in film plane and x is in-plane of film and vertical to y and z direction. (e) Shows the spectrum obtained on a smooth Kapton film without NWs with the same light incident and observing directions as (a) to (c).

yz plane. In our experiment, light was shone on the film along— z direction perpendicular to the surface of film. And light was received along $D1$ direction, $D2$ direction deviating 170° and 10° counterclockwise from y axis in yz plane respectively, and $D3$ direction deviating 10° from x axis in xz plane. The film shows different colors from blue, buff to deep yellow at different direction $D1$, $D2$ and $D3$. The scattering spectrum received along direction $D1$ shows strong reflection in wavelength range between 400–600 nm (Fig. 6(a)). While along $D2$ and $D3$ directions, the strongest reflection is concentrated in 550–1000 nm wavelength range (Figs. 6(b) and (c)). Compared with the scattering spectrum of an untreated smooth Kapton film (Fig. 6(e)), it can be concluded that the reflections between 550–1000 nm wavelength are mainly from the Kapton film. It indicates that the reflections between 400–600 nm wavelength come from the scattering by the structure of patterned oblique NW arrays.

To explain the effect of NW arrays on the scattering spectrum, we established the following model. As shown in Figure 7, parallel light shone vertically onto the surface, and was reflected by oblique NW arrays. Angle between incident light and reflected light was 2θ (θ is the obliquity of NWs) according to reflection law.

Figure 7 shows the specific optical path difference ($L_{BCD} - L_{AB}$) between two adjacent NWs. According to the principle of light interference, when the optical path

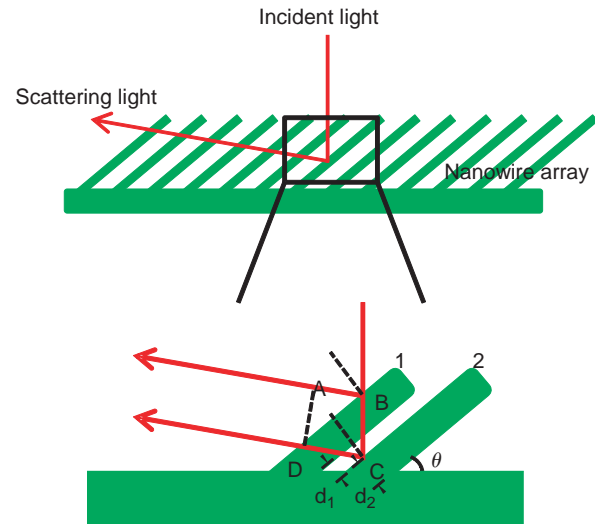


Fig. 7. The model to explain anisotropic scattering of light induced by the film with oblique NW array. When incident light is vertical to the film, it is scattered to a certain direction. And the interference of scattering light leads to enhancement of the light with certain wavelength at this direction.

difference equals to integral multiple of the wavelength, the maxima reflection is available, and when the optical path difference equal to half-integer multiple of the wavelength, the reflection reaches minimum. Here, we defined λ_1 , λ_2 , λ_3 as the wavelengths corresponded to the conditions that $L_{BCD} - L_{AB}$ equals to 1, 0.5 and 1.5 times of the wavelength, these wavelengths can be calculated with the following equations,

$$L_{BCD} - L_{AB} = 2d_1 \cos(\theta) + 2d_2 \sec(\theta)(n - \sin(\theta)^2) \quad (1)$$

$$\lambda_1 = L_{BCD} - L_{AB} \quad (2)$$

$$\lambda_2 = 2(L_{BCD} - L_{AB}) \quad (3)$$

$$\lambda_3 = \frac{2}{3}(L_{BCD} - L_{AB}) \quad (4)$$

Here d_1 is the distance along the substrate plane between two neighbor NWs, d_2 is the size of the NWs on the substrate, θ is the angle between NWs and the surface of the film, n is the refractive index of the NWs.

In our experiment, $d_1 = 39$ nm, $d_2 = 122$ nm, $\theta = 40^\circ$, and the refractive index of Kapton film is 1.7.²⁵ Substitute the above values to Eqs. (1)–(4), we get, $\lambda_1 = 469$ nm, $\lambda_2 = 938$ nm, $\lambda_3 = 313$ nm. The calculated result shows, the reflected light intensity will reach the highest value when the wavelength is 469 nm. And the intensity will decrease from highest to lowest as the wavelength increase/decrease from 469 nm to 938/313 nm. And this result fits well with the experimental result shown in Figure 6(a).

4. CONCLUSIONS

In summary, a SAIB method is developed to fabricate patterned oblique NW arrays of different materials.

The obliquity, diameter, length, and wire density of NWs are well controlled. Kapton film covered with patterned oblique NW array shows strong anisotropic optical property and different structural color in different directions, which has great potential in the application of gratings and biomimetics.

5. EXPERIMENTAL DETAILS

Synthesis of silica nanospheres:²⁶ First, 5 mL H₂O, 5 mL aqueous ammonia (25%–28%) and 40 mL ethanol were added in a triangular flask and stirred at an appropriate speed. Then, the flask was heated to 40 °C, and then dropwise 10 mL tetraethyl orthosilicate (TEOS) were added. After 6 hours reaction, silica nanospheres with average diameter about 250 nm were formed in the solution. The nanospheres were centrifuged and cleaned with water several times. Silica nanospheres with larger diameter were synthesized by the following method. First, solution with the same composition was reacted at the same stirring speed and temperature for 3 hours, and then a proper amount of H₂O and TEOS with volume ratio of 1:2 was added into the solution (TEOS was added dropwise, 5, 10, 20 mL TEOS for 308, 355, 425 nm silica nanospheres, respectively). After another 3 hours reaction, silica nanospheres with larger diameters were centrifuged and cleaned in the same way.

Dip-coating experiment: After drying in an oven, 5 g silica nanospheres and 0.1 g sodium dodecyl sulfate (SDS) were added into 100 mL deionized water, and then ultrasonically dispersed for more than one day. This solution was used in dip-coating later. Kapton and PET film was ultrasonic cleaned for several minutes in acetone and ethyl alcohol in order, and then rinsed in water to remove residual acetone and ethyl alcohol. The film was blow-dried by cleaning air. PANI and SU-8 resist was spin coated on a clean PET substrate and baked on a hot plate respectively. After all these steps, all polymer substrates were clean and could be used for dip-coating.

The solution shown above was put in a suitable vessel and the polymer substrate was dipped vertically in the solution for about 5 minutes. After the solution was stable, the substrate was pulled out from the solution with a uniform speed. By adjusting pulling speed, uniform monolayer silica nanospheres could form on surface of polymer substrate. Because the solution show different wetting ability on different polymer surface, different pulling speed was used in fabricating the monolayer nanospheres on different polymer films.

Ar⁺ ion bombardment: Polymer film with monolayer silica nanospheres on the surface were bombarded by Ar⁺ ion beam in an Ion Milling using a method reported in previous work.²³ Here accelerating voltage of Ar⁺ ions was 4 kV, and beam current was 200 μ A. Incident angle of Ar⁺ ion beam could be adjusted from 0–90° and the patterned

oblique NW arrays were obtained after bombarding under this condition for 20 mins.

Measurement of anisotropic scattering of light: In this experiment, incident light was provided by a miniature xenon lamp, and scattered light was measured by a spectrometer (AvaSpec-2048TEC). Incident angle and receiving direction could be adjusted as needed.

Acknowledgment: We gratefully acknowledge the financial support from NSFC (No. 50972053), Fok Ying Tung education foundation (131044), the Fundamental Research Funds for the Central Universities (No. Izujbky-2010-k01). And we thank Professor Qiang Wang for his help in measurement of scattering spectrum.

References and Notes

1. K. Autumn, Y. A. Liang, S. T. Hsieh, W. Zesch, W. P. Chan, T. W. Kenny, R. Fearing, and R. J. Full, *Nature* 405, 681 (2000).
2. S. N. Gorb, R. G. Beutel, E. V. Gorb, Y. Jiao, V. Kastner, S. Niederegger, V. L. Popov, M. Scherge, U. Schwarz, and W. Vötsch, *Integr. Comp. Biol.* 42, 1127 (2002).
3. M. P. Murphy, B. Aksak, and M. Sitti, *Small* 5, 170 (2009).
4. M. Gleiche, L. F. Chi, and H. Fuchs, *Nature* 403, 173 (2000).
5. T.-I. Kim and K. Y. Suh, *Soft Matter* 5, 4131 (2009).
6. K.-H. Chu, R. Xiao, and E. N. Wang, *Nat. Mater.* 9, 413 (2010).
7. N. A. Malvadkar, M. J. Hancock, K. Sekeroglu, W. J. Dressick, and M. C. Demirel, *Nat. Mater.* 9, 1023 (2010).
8. D. Xia and S. R. J. Brueck, *Nano Lett.* 8, 2819 (2008).
9. S. Tawfik, M. De Volder, D. Copic, S. J. Park, C. R. Oliver, E. S. Polsen, M. J. Roberts, and A. J. Hart, *Adv. Mater.* 24, 1628 (2012).
10. J. K. Gansel, M. Thiel, M. S. Rill, M. Decker, K. Bade, V. Saile, G. von Freymann, S. Linden, and M. Wegener, *Science* 325, 1513 (2009).
11. S. Kinoshita, S. Yoshioka, and K. Kawagoe, *Proc. R. Soc. B* 269, 1417 (2002).
12. S. Yoshioka and S. Kinoshita, *Proc. R. Soc. B* 271, 581 (2004).
13. S. N. Gorb, *Proc. R. Soc. B* 266, 525 (1999).
14. S. N. Gorb, *Int. J. Insect Morphol. Embryol.* 27, 205 (1998).
15. R. J. Kennedy, *Nature* 227, 736 (1970).
16. C. Y. Chen, J. H. Huang, K. Y. Lai, Y. J. Jen, C. P. Liu, and J. H. He, *Opt. Express* 20, 2015 (2012).
17. Y. Zhao, D. Ye, G.-C. Wang, and T.-M. Lu, *Designing Nanostructures by Glancing Angle Deposition*, edited by A. Lakhtakia and S. Maksimenko, SPIE, San Diego (2003), Vol. 5219, p. 59.
18. K. Robbie, M. J. Brett, and A. Lakhtakia, *Nature* 384, 616 (1996).
19. Y. Shen, J. I. Hong, Z. C. Peng, H. Fang, S. Zhang, S. X. Dong, R. L. Snyder, and Z. L. Wang, *J. Phys. Chem. C* 114, 21277 (2010).
20. Y. Shen, J. I. Hong, S. Xu, S. S. Lin, H. Fang, S. Zhang, Y. Ding, R. L. Snyder, and Z. L. Wang, *Adv. Funct. Mater.* 20, 703 (2010).
21. M. K. Choi, H. Yoon, K. Lee, and K. Shin, *Langmuir* 27, 2132 (2011).
22. T. I. Kim, H. E. Jeong, K. Y. Suh, and H. H. Lee, *Adv. Mater.* 21, 2276 (2009).
23. W. Wu, L. Cheng, S. Bai, Z. L. Wang, and Y. Qin, *Adv. Mater.* 24, 817 (2012).
24. Y. Lu, R. Ganguli, C. A. Drewien, M. T. Anderson, C. J. Brinker, W. Gong, Y. Guo, H. Soye, B. Dunn, M. H. Huang, and J. I. Zink, *Nature* 389, 364 (1997).
25. L. K. Massey (ed.), *Film Properties of Plastics and Elastomers: A Guide to Non-Wovens in Packaging Applications*, William Andrew, New York (2004).
26. G. H. Bogush, M. A. Tracy, and C. F. Zukoski Iv, *J. Non-Cryst. Solids* 104, 95 (1988).